The complex local mean decomposition

Cheolsoo Park [a,*], David Looney [a], Marc M. Van Hulle [b], Danilo P. Mandic [a]

[a] *Department of Electrical and Electronic Engineering, Imperial College London, London SW7 2BT, UK*
[b] *Laboratorium voor Neuro- en Psychofysiologie, K.U.Leuven, Campus Gasthuisberg, Herestraat 49, B-3000 Leuven, Belgium*

ARTICLE INFO

ABSTRACT

The local mean decomposition (LMD) has been recently developed for the analysis of time series which have nonlinearity and nonstationarity. The smoothed local mean of the LMD surpasses the cubic spline method used by the empirical mode decomposition (EMD) to extract amplitude and frequency modulated components. To process complex-valued data, we propose complex LMD, a natural and generic extension to the complex domain of the original LMD algorithm. It is shown that complex LMD extracts the frequency modulated rotation and envelope components. Simulations on both artificial and real-world complex-valued signals support the analysis.

© 2010 Elsevier B.V. All rights reserved.

1. Introduction

Standard signal analysis techniques, such as Fourier analysis, are based on assumptions of linearity and stationarity of the signal. Since most real-world signals contain nonlinearity[1] and nonstationarity,[2] time–frequency analysis techniques such as the short time Fourier transform (STFT) and the wavelet transform (WT) have attracted considerable attention. However, their application is often limited since they are based on a projection onto a predefined set of basis functions [3]. Recent research on signal decomposition has been based on fully data-driven techniques, exploratory data analysis (EDA) [4]. One such technique is empirical mode decomposition (EMD), which is a fully adaptive approach that decomposes the signal into a finite set of AM/FM components [5]. EMD makes no prior assumptions on the data and, as such, it is ideal for the analysis of nonlinear and nonstationary data. Due to the monocomponent nature of its decomposition, the Hilbert transform can be applied to obtain an analytic representation for the signal, from which the instantaneous frequency (IF) and instantaneous amplitude (IA) can be determined. EMD has found numerous applications, including radar technology [6] and biomedical engineering [7–9]. However, the use of cubic splines and the Hilbert transform in the EMD process induces a loss of amplitude and frequency information [10], as illustrated by an often erratic or negative IF. To this end, the local mean decomposition (LMD) was recently introduced [10]. LMD uses smoothed local means to determine a more credible and reliable IF directly from the oscillations within the signal without the Hilbert transform. Its application has been originally illustrated on electroencephalogram (EEG) [10], and in [11,12] it was shown how LMD facilitated enhanced analysis compared to EMD in rub-impact fault diagnosis.

Real-valued data sources, for which both amplitude and phase information are significant, can be conveniently represented by complex algebra, for instance, in medical devices (MRI and Ultrasonography), telecommunication and sonar. In addition, the extension to the complex domain makes it straightforward to combine real-valued data from different sources, which is needed in multichannel data processing [13]. The original LMD algorithm was introduced for real-valued data, and this paper proposes its generic extension to complex and bivariate signals.

2. Local mean decomposition and complex local mean decomposition

The real-valued LMD algorithm is described in Table. 1. The main principle of LMD is decomposing a given signal into pairs of frequency modulated signals and envelope components known as

---

* Corresponding author.
  E-mail addresses: cheolsoo.park07@imperial.ac.uk (C. Park),
david.looney06@imperial.ac.uk (D. Looney),
marc@neuro.kuleuven.be (M.M. Van Hulle),
d.mandic@imperial.ac.uk (D.P. Mandic).

[1] A linear signal is one which cannot be generated by a linear time-invariant system (nonlinearity in the sense of non-Gaussianity [1,2]).
[2] If a signal is generated by time-variable dynamics, it is said to be nonstationary [1].

Table 1
Local mean decomposition.

1. From the original signal $x(t)$, determine the mean value, $m_{i,k}$, by calculating the mean of the successive maximum and minimum $n_{k,c}$ and $n_{k,c+1}$, where c is the index of the extrema. 'i' and 'k' denote the order of PF and the iteration number in a process of PF. The local magnitude, $a_{i,k}$ is determined by the difference between the successive extrema:

$$m_{i,k,c} = \frac{n_{k,c} + n_{k,c+1}}{2}, \quad a_{i,k,c} = \frac{|n_{k,c} - n_{k,c+1}|}{2}$$

2. Interpolate straight lines of local mean and local magnitude values between successive extrema, $m_{i,k}(t)$ and $a_{i,k}(t)$.
3. Smooth the interpolated local mean and local magnitude using moving average filter, $\tilde{m}_{i,k}(t)$ and $\tilde{a}_{i,k}(t)$.
4. Subtract the smoothed mean signal from the original signal, $x(t)$:

$$h_{i,k}(t) = x(t) - \tilde{m}_{i,k}(t)$$

5. Get the frequency modulated signal, $s_{i,k}(t)$, by dividing $h_{i,k}(t)$ by $\tilde{a}_{i,k}(t)$:

$$s_{i,k}(t) = \frac{h_{i,k}(t)}{\tilde{a}_{i,k}(t)}$$

6. Check whether $s_{i,k}(t)$ is a normalised frequency-modulated signal ($\tilde{a}_{i,k}(t)$ is close to 1), then go to step 9.
7. If not, multiply $\tilde{a}_{i,k}(t)$ by $\tilde{a}_{i,k-1}(t)$ and go back to the first step to repeat the same procedure for $s_{i,k}$.
8. Envelope function, $\tilde{a}_i(t)$, can be derived by multiplying all $\tilde{a}_{i,k}(t)$ until $\tilde{a}_{i,k}(t)$ equals one:

$$\tilde{a}_i(t) = \tilde{a}_{i,1}(t) \times \tilde{a}_{i,2}(t) \times \tilde{a}_{i,3}(t) \times \cdots \times \tilde{a}_{i,l}(t) = \prod_{q=1}^{l} \tilde{a}_{i,q}(t)$$

(l: maximum iteration number)
9. Using the envelope function, $\tilde{a}_i(t)$, and the final frequency modulated signal, $s_{i,l}(t)$, derive PF by their multiplication $PF_i = \tilde{a}_i(t) \times s_{i,l}(t)$
10. Subtract $PF_i(t)$ from $x(t)$

$$u_i(t) = x(t) - PF_i$$

Then the smoothed data, u_i, is treated as new input, $x(t)$, and the procedure is repeated from steps 1 to 9, until $u_i(t)$ becomes a monotonic function
11. From the frequency modulated signal, an instantaneous phase can be calculated:

$$\phi_i(t) = arccos(s_{i,l}(t))$$

12. The phase data unwrapped and its differentiation defines the IF:

$$w_i(t) = \frac{d\phi_i}{dt}$$

local magnitude functions. Firstly, the local mean of the signal is obtained by interpolating mean values of successive extrema using piecewise constant interpolation and applying a moving average filter. It is this process of determining the local mean function that makes LMD different from EMD [10]. In a similar fashion, the local magnitude function is determined by interpolating the absolute value of differences between successive extrema and smoothing using a moving average filter. The local mean is subtracted from the original signal and then the result is divided by the local magnitude function in order to obtain the frequency modulated signal. This process is repeated on the frequency modulated signal until its envelope is uniform. Multiplying all envelope estimates during this process gives the local magnitude function. The product of this local magnitude signal and the frequency modulated signal determines the first product function (PF). The PF is subtracted from the original data, and the same process is repeated so as to decompose the rest of the signal into a set of PFs and a monotonic trend.

The local magnitude function represents the IA, and the IF can be directly derived from the frequency modulated signal without the need for applying the Hilbert transform and deriving an analytic representation. The IA and IF calculated using LMD are more stable and precise than those obtained by EMD because LMD uses smoothed local means and local magnitudes which facilitate a more natural decomposition than that using the cubic spline approach of EMD [10]. In this way, it has been previously illustrated [10] how LMD gives a more localised time–frequency estimate for EEG.

To illustrate the advantages of standard real-valued LMD it was applied to a neuronal spike stream used in neuronal spike modeling for brain computer interface (BCI), shown in Fig. 1. This time series was generated by the tool described in [14]. Fig. 2(a) shows the time–frequency representation (TFR) composed of the LMD PFs, whereas Fig. 2(b) shows the TFR generated by EMD. As seen in the figures, both decomposition algorithms detect the considerable
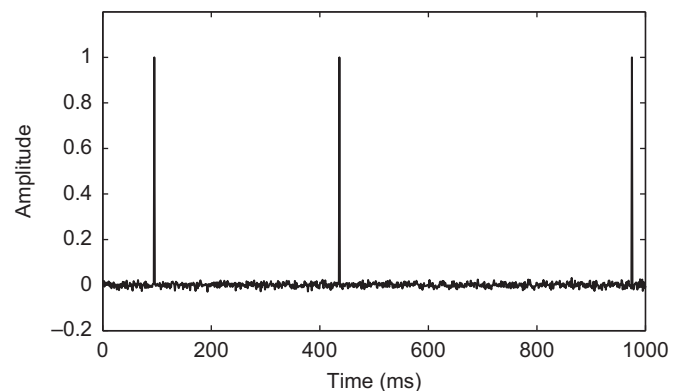
Fig. 1. Neuronal spike stream. The spike signal is generated with 10 kHz sampling frequency for a duration of 1 s. This neuronal spike signal has nonlinearity, and has substantial and abrupt changes of frequency at the locations of spikes.

change in frequency surrounding the spikes. However, the LMD spectrum is much sharper and concentrated in time compared to the EMD spectrum. The cubic spline approach of EMD as well as an IF that is derived from a time-varying envelope can result in the loss of frequency and amplitude information of the spikes.

In order to extend the original LMD to the complex domain, the basic steps of LMD should operate directly in $\mathbb{C}$. However, a significant obstacle is that there is no ordering of numbers in $\mathbb{C}$, which makes it difficult to define local extrema. In the case of EMD, it has been extended to the $\mathbb{C}$ domain in three different ways, 'rotation invariant empirical mode decomposition (RIEMD)' [15], 'complex empirical mode decomposition (CEMD)' [16] and 'bivariate empirical mode decomposition (BEMD)' [17]. Among these, the framework of RIEMD and BEMD was exploited to develop the complex version of LMD. In the three dimensional (3D) plane of

a

b
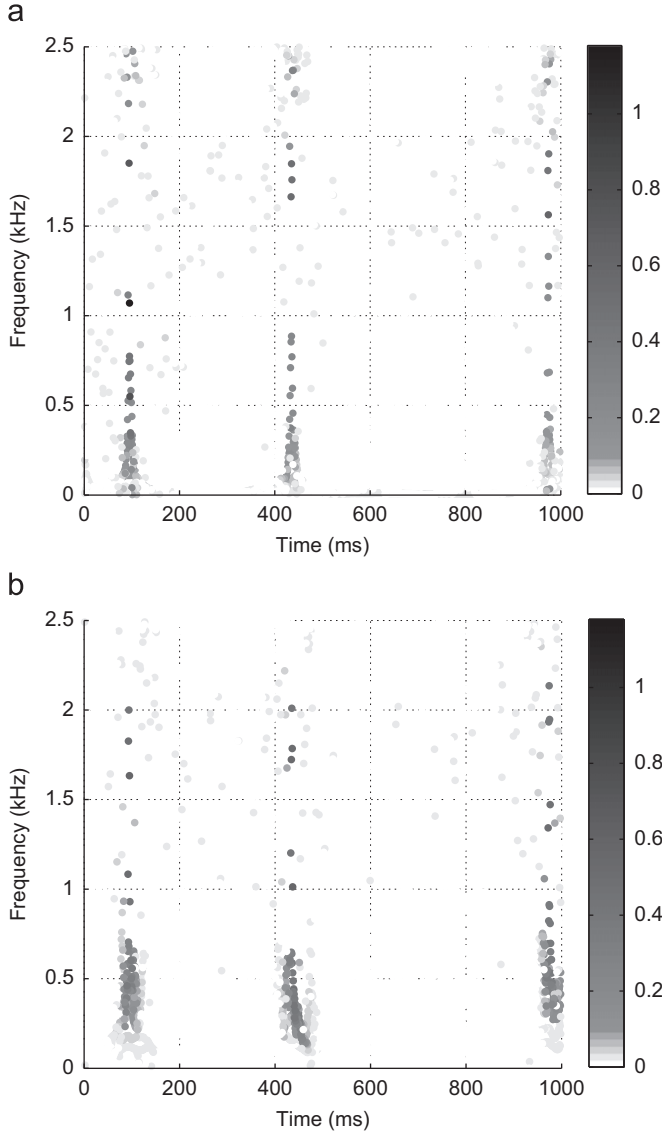
Fig. 2. Comparison of LMD and EMD in the analysis of the neuronal spike signals shown in Fig. 1. LMD result contains sharper and more concentrated frequency components around the spikes compared to EMD. (a) Time–frequency representation using LMD. (b) Time–frequency representation using EMD.

Fig. 3, the extrema of the complex data are found based on the intersect of the 3D tube in the top, bottom, left and right directions. The local mean and local magnitude of the complex signal can be extracted from the extrema on the four sides. To achieve this, the complex signal is projected into two directions, 0 and $\pi/2$, so that the projected result becomes a two-dimensional signal.[3] Projections of a complex signal $z = x + jy$ in the directions 0 and $\pi/2$ are given by

$$\mathrm{Re}(e^{j(-0)}(x+jy)) = \mathrm{Re}((\cos 0 + j\sin 0)(x+jy)) = \mathrm{Re}(x+jy) = x$$

$$\mathrm{Re}(e^{j(-\pi/2)}(x+jy)) = \mathrm{Re}\left(\left(\cos\left(-\frac{\pi}{2}\right) + j\sin\left(-\frac{\pi}{2}\right)\right)(x+jy)\right)$$
$$= \mathrm{Re}(-j(x+jy)) = y$$

---

[3] Since calculating the local mean and the local magnitude for complex LMD is based on projections in a 3D plane, increasing the number of projection directions, for example $\pi/4$ and $3\pi/4$, would provide a more accurate estimate.
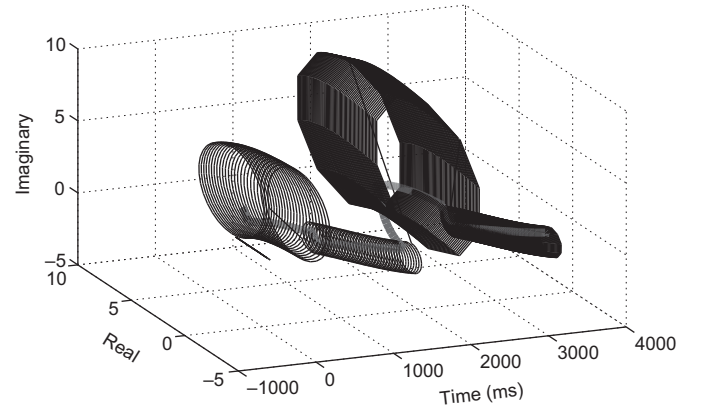
Fig. 3. Complex signal composed of sine and cosine signals. The frequencies of the first two complex signals are 1 kHz and the frequencies of the other two tubes are 3 kHz. In addition, all of the complex signals include a 7 Hz low frequency component. The grey line illustrates the local mean of the complex signal.

For each projection of the complex signal, the smoothed local mean and local magnitude of x and y are then calculated in the same way as the original LMD. The smoothed local means for each projection are multiplied by e^{j0} and $e^{j\pi/2}$ according to the direction in which they are obtained and averaged, to construct a single complex local mean value. With the so-obtained complex-valued mean in $\mathbb{C}$, the rest of the procedure is the same as the original LMD. The complex LMD algorithm is summarized in Table 2.

3. Simulations and discussion

In order to illustrate the operation of the complex LMD, several simple rotational signals were used, which were made by concatenating sinusoids with different frequencies. Fig. 3 shows four different complex signals created using

$$f_1 = 1\ \text{kHz}, \quad f_2 = 3\ \text{kHz}, \quad f_3 = 7\ \text{Hz}$$

$$T_1(t) = 3 \times (\cos(2\pi f_1 t) + j\sin(2\pi f_1 t) + \cos(2\pi f_3 t))$$

$$T_2(t) = \cos(2\pi f_1 t) + j\sin(2\pi f_1 t) + \cos(2\pi f_3 t)$$

$$T_3(t) = 5 \times (\cos(2\pi f_2 t) + j\sin(2\pi f_2 t) + \cos(2\pi f_3 t))$$

$$T_4(t) = \cos(2\pi f_2 t) + j\sin(2\pi f_2 t) + \cos(2\pi f_3 t)$$

The thick gray line in the middle of the complex signals represents the smoothed mean value calculated during the process of envelope estimation, and follows closely the actual mean. Fig. 4 shows the result of applying the complex LMD to the signal shown in Fig. 3. Fig. 4(a) shows the frequency modulated rotation of the first PF and Fig. 4(b) shows its local magnitude function. It can be seen that the amplitude of the envelope in the frequency modulated signal is approximately unity and it contains slow rotations and fast rotations reflecting the rotations of the original data. The envelope signal in Fig. 4(b) contains the same amplitude as Fig. 3. All PFs derived by complex LMD are shown in Fig. 5. Before this simulation, only two or three PFs were anticipated because the original signal was made by simple sinusoidal signals. However, due to the discontinuities in the complex data, high frequency components were introduced, and LMD produced nine PFs and a redundant function. The first PF represented the two high frequency rotations, 1 and 3 kHz, whereas the last PF, PF9, contained the low frequency component, that was the 7 Hz sine signal. This problem could be alleviated by increasing the number of projection directions used to estimate the local mean.

Table 2
Complex local mean decomposition.

1. Project the complex signal z(t) on direction 0. (t:time)

$$p_0(t) = Re(e^{-j0} \cdot z(t))$$

2. Find the extrema of $p_0(t)$. With the extrema, calculate the smoothed mean, $\tilde{m}_{0(i,k)}(t)$, and local magnitude, $\tilde{a}_{0(i,k)}(t)$, like original LMD (Table 1).
   (i: number of PF, k: iteration number)
3. Go back to the first process and project the complex signal z(t) on direction $\pi/2$.

$$p_{\pi/2}(t) = Re(e^{-j\pi/2} \cdot z(t))$$

4. Calculate the smoothed mean, $\tilde{m}_{(\pi/2)(i,k)}(t)$, and local magnitude, $\tilde{a}_{(\pi/2)(i,k)}(t)$.
5. Multiply the smoothed means by e^{j0} and $e^{j\pi/2}$ according to their direction:

$$mc_{0(i,k)}(t) = e^{j0} \cdot \tilde{m}_{0(i,k)}(t), \quad mc_{(\pi/2)(i,k)}(t) = e^{j\pi/2} \cdot \tilde{m}_{(\pi/2)(i,k)}(t)$$

6. Compute the complex-valued mean using the smoothed means, $mc_{0(i,k)}$ and $mc_{(\pi/2)(i,k)}$.

$$M_{i,k}(t) = mc_{0(i,k)}(t) + mc_{(\pi/2)(i,k)}(t)$$

7. Subtract the mean, $M_{i,k}$, from z(t):

$$H_{i,k}(t) = z(t) - M_{i,k}(t)$$

8. Calculate the frequency modulated rotation, $s_{0(i,k)}(t)$ and $s_{(\pi/2)(i,k)}(t)$, using the local magnitudes:

$$s_{0(i,k)}(t) = \frac{Re(e^{-j0} \cdot H_{i,k}(t))}{\tilde{a}_{0(i,k)}(t)}, \quad s_{(\pi/2)(i,k)}(t) = \frac{Re(e^{-j\pi/2} \cdot H_{i,k}(t))}{\tilde{a}_{(\pi/2)(i,k)}(t)}$$

9. Check whether $\tilde{a}_{0(i,k)}(t)$ and $\tilde{a}_{(\pi/2)(i,k)}(t)$ are equal to 1
10. If one of them is not, multiply $\tilde{a}_{0(i,k)}(t)$ and $\tilde{a}_{(\pi/2)(i,k)}(t)$ by $\tilde{a}_{0(i,k-1)}(t)$ and $\tilde{a}_{\pi/2(i,k-1)}(t)$ and go to the first step:

$$a_{0(i)}(t) = \tilde{a}_{0(i,1)}(t) \cdots \tilde{a}_{0(i,2)}(t) \cdot \tilde{a}_{0(i,3)}(t) \cdots \cdots \tilde{a}_{0(i,l)}(t) = \prod_{q=1}^{l} \tilde{a}_{0(i,q)}(t)$$

$$a_{\pi/2(i)}(t) = \tilde{a}_{(\pi/2)(i,1)}(t) \cdot \tilde{a}_{(\pi/2)(i,2)}(t) \cdot \tilde{a}_{(\pi/2)(i,3)}(t) \cdots \cdots \tilde{a}_{(\pi/2)(i,l)}(t) = \prod_{q=1}^{l} \tilde{a}_{(\pi/2)(i,q)}(t)$$

   (l: maximum iteration number until $\tilde{a}_{0(i,k)}(t)$ and $\tilde{a}_{(\pi/2)(i,k)}(t)$ become equal to 1)
11. Derive the complex PF:

$$cPF_i(t) = a_{0(i)}(t) \cdot s_{0(i,l)}(t) \cdot e^{j0} + a_{(\pi/2)(i)}(t) \cdot s_{(\pi/2)(i,l)}(t) \cdot e^{j\pi/2}$$

12. Subtract $cPF_i(t)$ from z(t), and then go to step 1 with the remain.
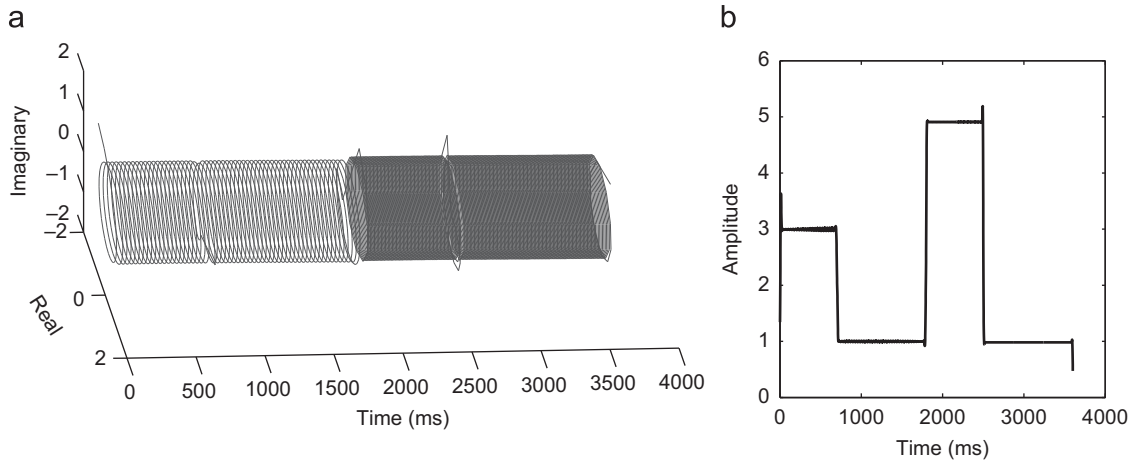
Fig. 4. A PF by complex LMD consists of a frequency modulated rotation and local magnitude function. (a) The frequency modulated rotation produced by complex LMD. (b) The envelope signal for the complex signal.

The performance of complex LMD and BEMD are compared in the next simulation, following observations made by [12] for the real-valued LMD. A complex signal was generated by combining two different Duffing wave signals with additional trend components, $s_1(t)$ and $s_2(t)$, given by

$$s_1(t) = e^{-t/256}\cos\left[\frac{\pi}{64}\left(\frac{t^2}{512} + 32\right) + 0.3\sin\left(\frac{\pi}{32}\left(\frac{t^2}{512} + 32\right)\right)\right] + 0.06e^{2t/1024}$$

$$s_2(t) = e^{-t/512}\cos\left[\frac{\pi}{64}\left(\frac{t^2}{512} + 32\right) + 0.3\sin\left(\frac{\pi}{32}\left(\frac{t^2}{512} + 32\right)\right) + \frac{\pi}{8}\right] + 0.03e^{2t/1024}$$

Note that a phase difference of $\pi/8$ exists between the Duffing wave signals contained in $s_1(t)$ and $s_2(t)$ each has an IF given by

$$f(t) = \frac{\varphi'(t)f_s}{2\pi} = \frac{t}{32768}\left(1 + 0.6\cos\left[\frac{\pi}{32}\left(\frac{t^2}{512} + 32\right)\right]\right)$$

When the complex-valued signal, $s_1(t) + js_2(t)$ (shown in Fig. 6(a)), is decomposed using complex LMD and BEMD, the pure Duffing waves without trend components are extracted in the real and imaginary parts of the first PF and the first IMF, which are shown in Fig. 6(b) and (c). The IF estimations calculated from the first PF and the first IMF are compared with the true IF for the real and imaginary parts in
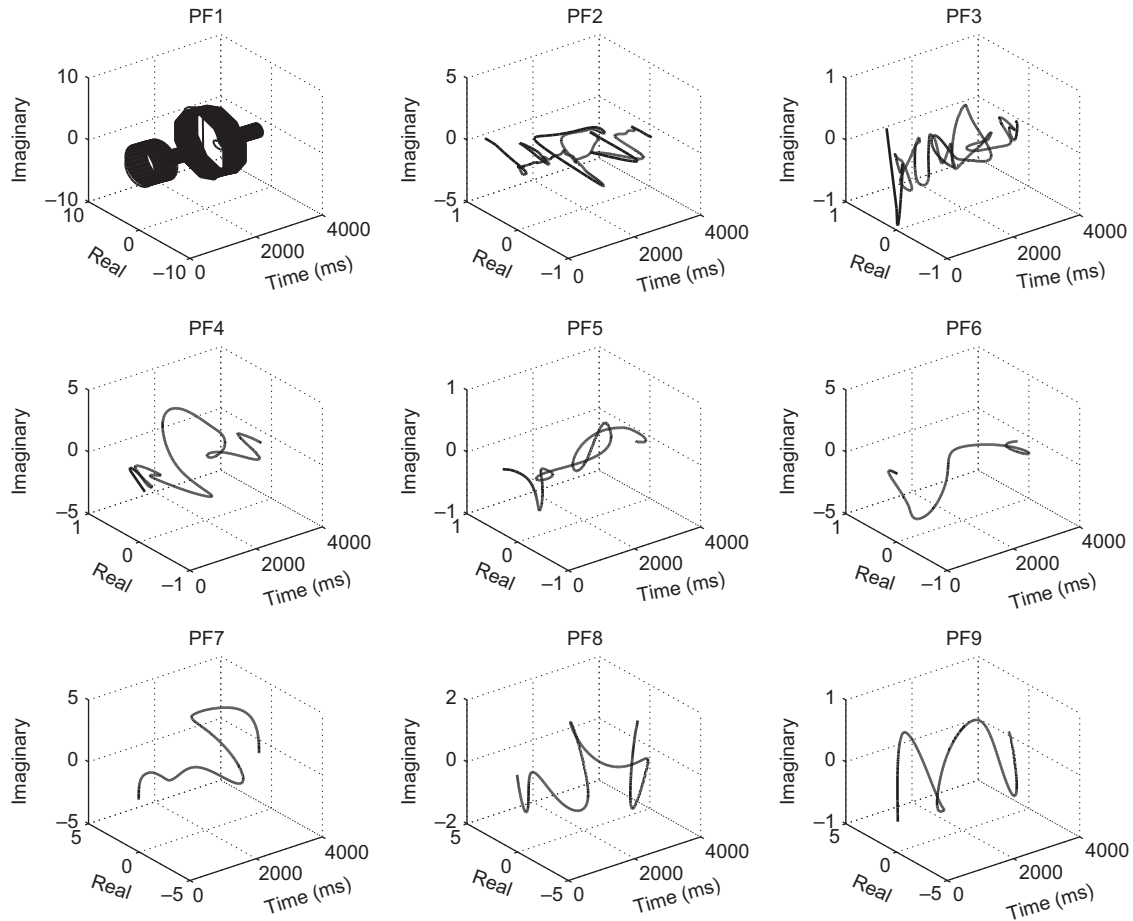
Fig. 5. PFs of the complex data in Fig. 3. Note that PF1 has 1 and 3 kHz rotations contained in the original data and PF9 contains the 7 Hz low frequency component.
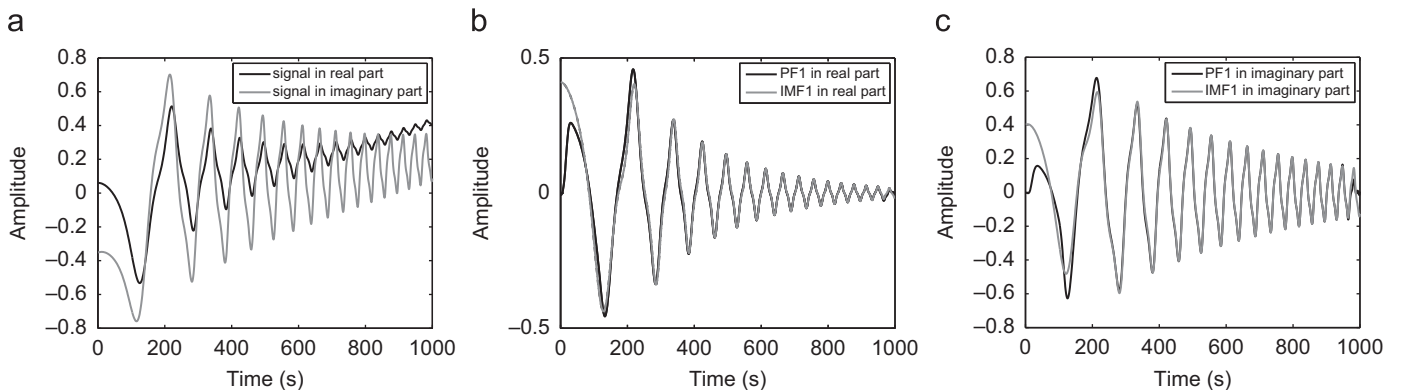
Fig. 6. Decomposition of a complex signal generated by combining two Duffing waves and an additional complex low frequency trend. The first PF and IMF in real and imaginary parts contain pure Duffing waves without trend. (a) Complex signal. (b) PF1 and IMF1 in real part. (c) PF1 and IMF1 in imaginary part.

Figs. 7(a) and (c) respectively. Note the IFs of complex LMD are closer to the true IF and the errors are smaller than those of BEMD for both the real and imaginary parts.

For the last experiment, Fig. 8(a) shows two spiking neuron time series—the first spike is the same signal as that shown in Fig. 1 and the other is also generated by the tool described in [14]. The sampling frequency was 10 kHz and the duration was 1 s. With the two real-valued time series ($x_1(t)$ and $x_2(t)$), a complex signal was constructed as $z(t) = x_1(t) + jx_2(t)$ (see Fig. 8(b)). The complex signal $z(t)$ was decomposed into complex PFs by complex LMD, and the real and imaginary parts of the PFs were separated from the results,

as shown in Fig. 9. Figs. 9(a) and (b) show respectively the real and imaginary parts of the PFs. Note that the real parts of PFs corresponded to $x_1(t)$, the real part of $z(t)$, and the imaginary parts of PFs were related to $x_2(t)$, the imaginary part of $z(t)$.

The component-wise TFRs were calculated for $z(t)$ in order to illustrate the advantages of complex LMD over BEMD. Figs. 10 and 11 show the TFR comparison between the complex LMD and the BEMD for the real and imaginary parts. The time–frequency characteristics of the BEMD approach (Figs. 10(b) and 11(b)) were less concentrated around the spikes than those of the complex LMD approach (Figs. 10(a) and 11(a)). In BEMD, the cubic splines were
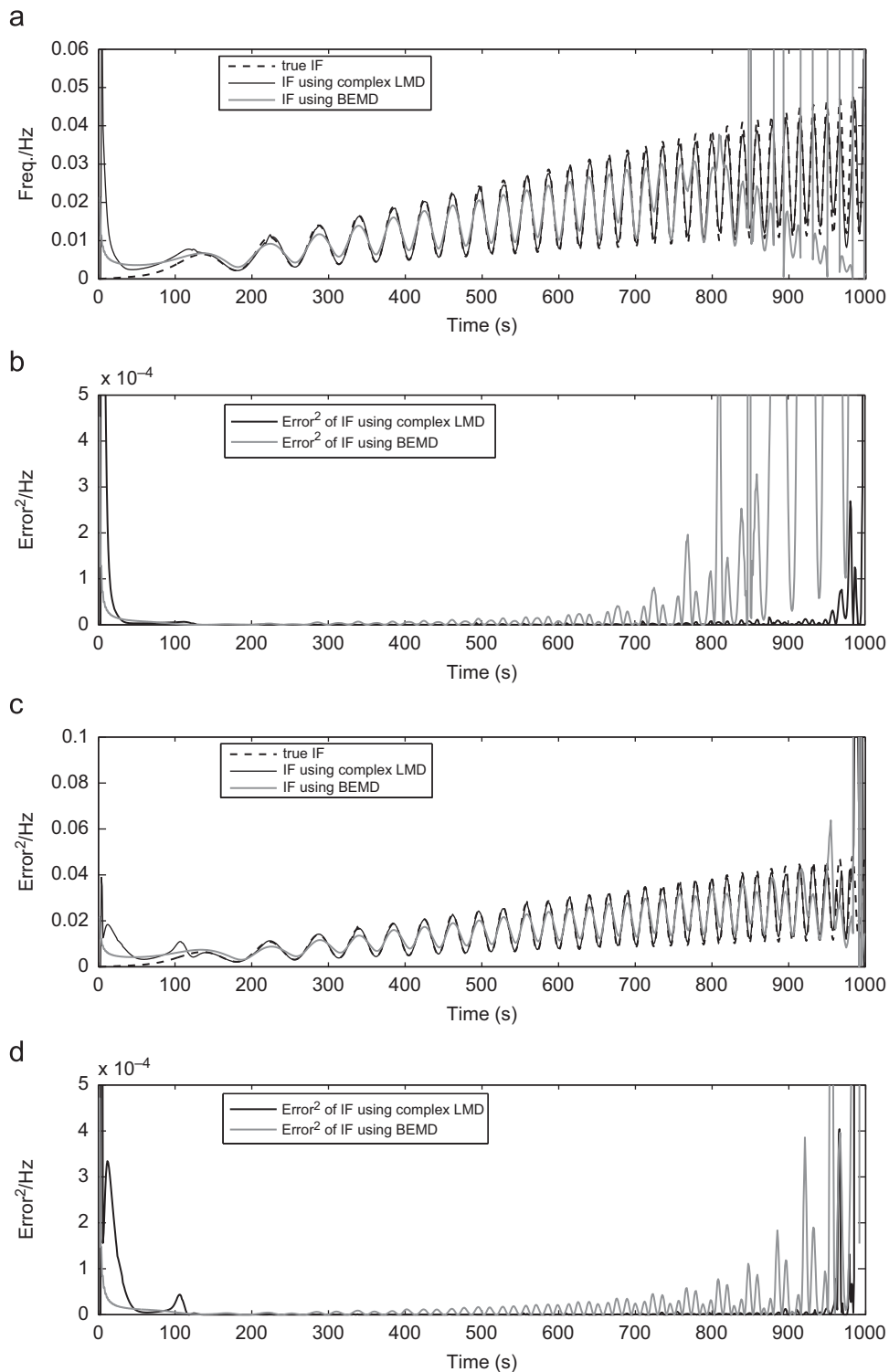
Fig. 7. The comparison of IFs estimated by 1st PF and IMF of a complex signal containing Duffing waves, Fig. 6(b) and (c). IFs derived by PF, in both the real and imaginary parts, are always closer to true values than those obtained using BEMD. (a) IFs from the real parts of PF1 and IMF1. (b) Squared errors between true and estimated IFs from the real parts of PF1 and IMF1. (c) IFs from the imaginary parts of PF1 and IMF1. (d) Squared errors between true and estimated IFs from the imaginary parts of PF1 and IMF1.

used, which caused a loss of amplitude and frequency information. The complex LMD provided a more robust estimate of IF owing to the smoothed local mean functions.

Future extension will include the development of a multivariate version of LMD following recent multivariate extensions of empirical mode decomposition [18], recently developed by extending bivariate and trivariate EMD [19].

4. Conclusions

We have introduced the complex local mean decomposition (LMD) by extending the original real-valued LMD algorithm to the complex domain. The proposed complex LMD approach is a natural and generic extension of the real-valued LMD. This way, the data are analyzed based on smoothed local means and local magnitudes
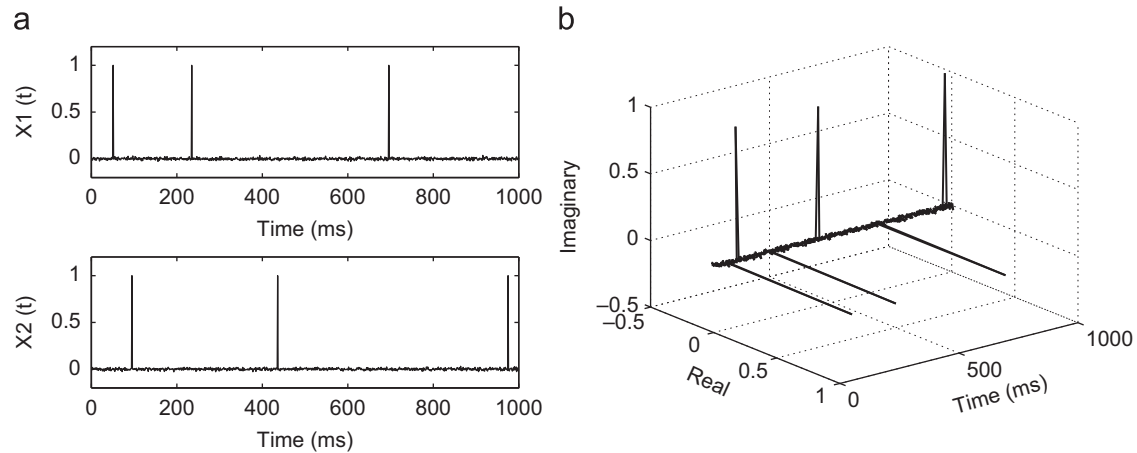
Fig. 8. 1D and 2D representations of an artificial complex signal composed of two neuronal spike signals. (a) Two neuronal spike signals. (b) Complex-valued representation. (c) PF1 and IMF1 in imaginary part.
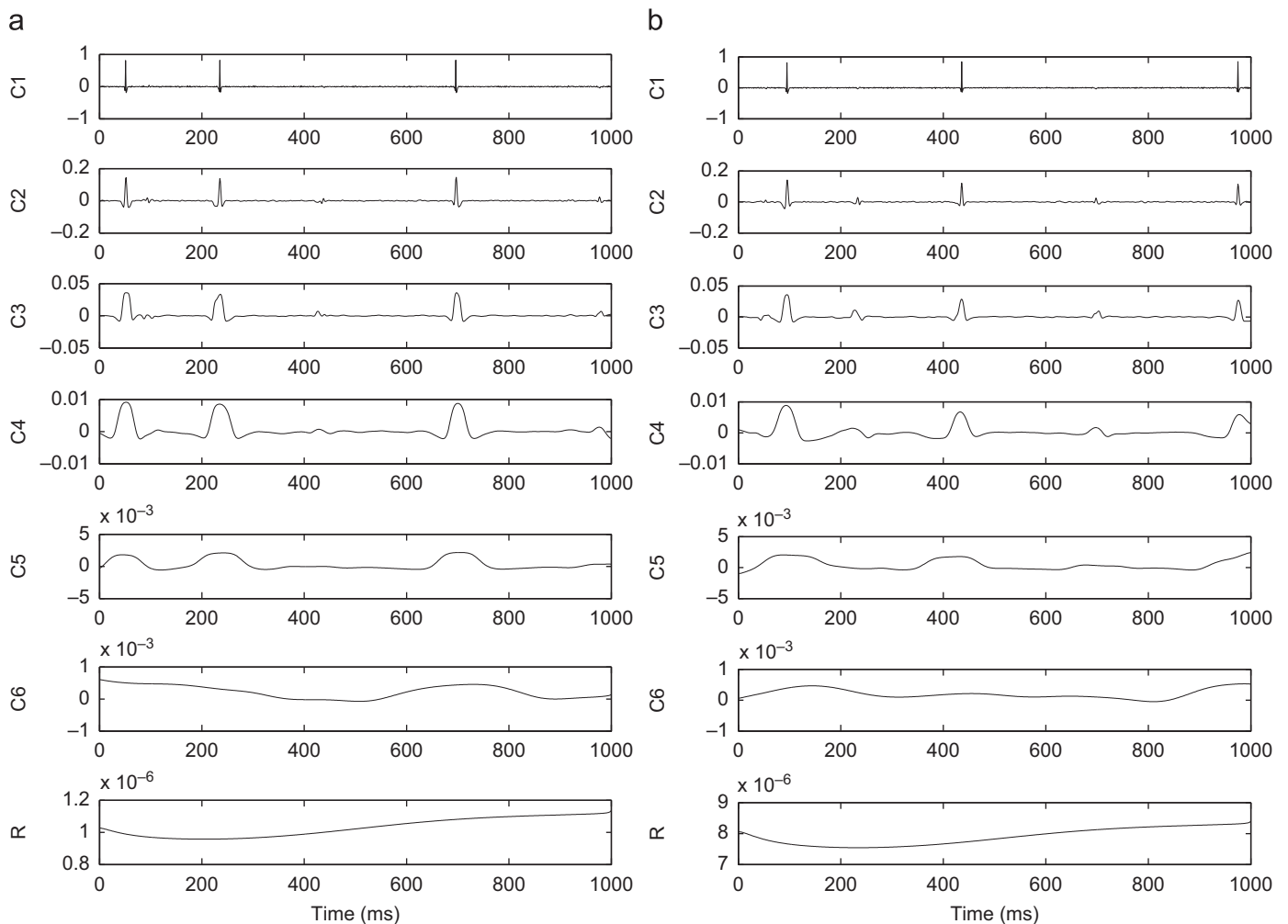
Fig. 9. The complex PFs of spikes, $z(t)=x_1(t)+jx_2(t)$, by complex LMD. (a) PFs corresponding to the real part of $z(t)$. (b) PFs corresponding to the imaginary part of $z(t)$.

rather than the cubic spline approach of bivariate EMD. Another advantage of complex LMD is that the IF from the frequency modulated rotation can be extracted directly without a Hilbert transformation, which can make the IF erratic [10]. Thus, the LMD has the potential to extract more accurate information about amplitude and frequency from data than the EMD approach. Simulations on neuronal spike trains illustrate how the proposed LMD extension retains the advantages of the original real-valued algorithm in the complex domain, facilitating highly localised time–frequency analysis.
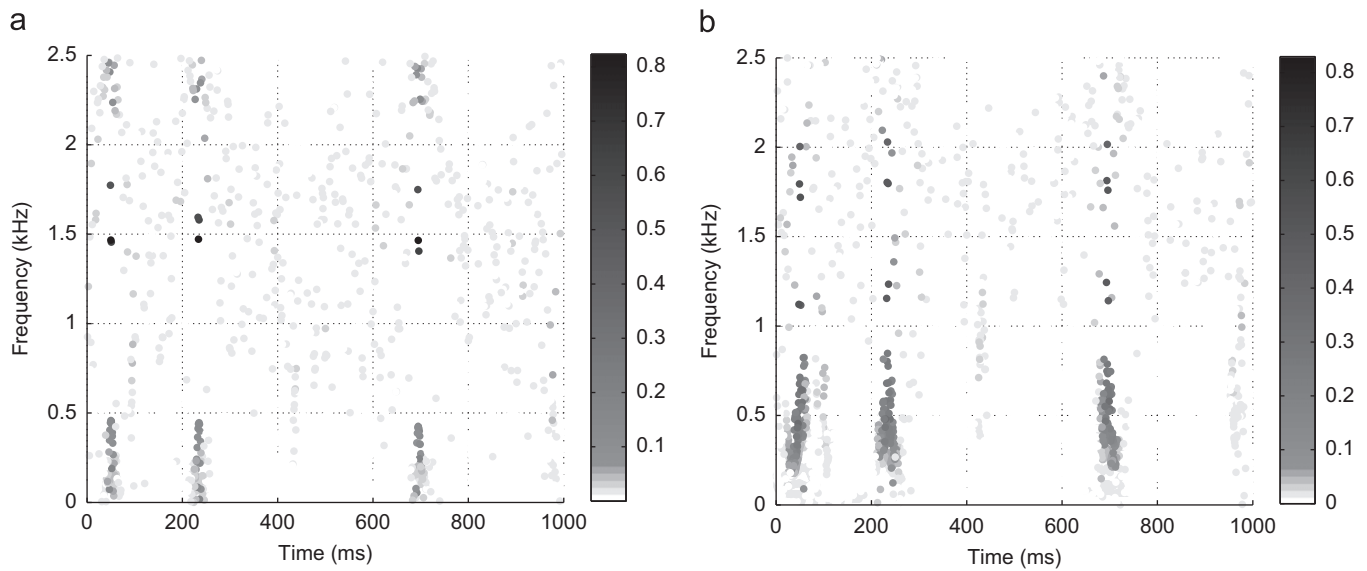
Fig. 10. Comparison of the time–frequency representations obtained using the real part of complex LMD and BEMD. The frequency components of the complex LMD provide more localised results than those using BEMD. (a) Time–frequency representation of the real part of complex LMD. (b) Time–frequency representation of the real part of BEMD.
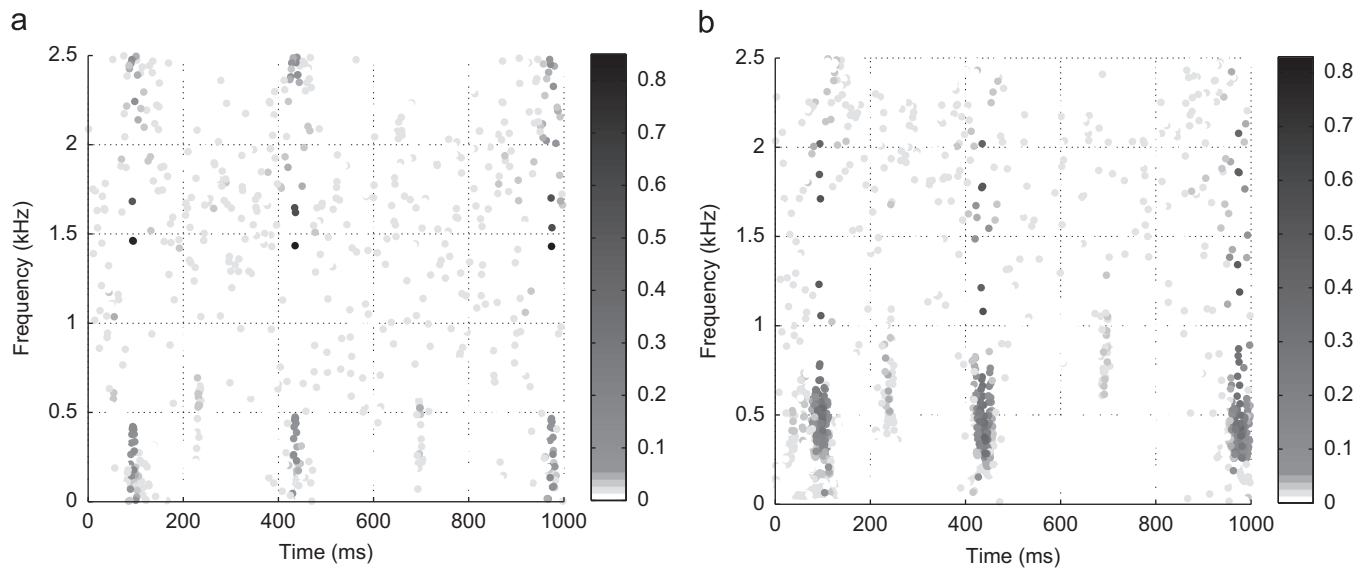
Fig. 11. Comparison of the time–frequency representations obtained using the imaginary part of complex LMD and BEMD. The frequency components of the complex LMD provide more localised results than those using BEMD. (a) Time–frequency representation of the imaginary part of complex LMD. (b) Time–frequency representation of the imaginary part of BEMD.

Acknowledgment

References

[1] T. Schreiber, Interdisciplinary application of nonlinear time series methods, Physics Reports 308 (1) (1998) 1–64.

[2] T. Schreiber, A. Schmitz, Discrimination power of measures for non-linearity in a time series, Physical Review E 55 (5) (1997) 5443–5447.

[3] D. Mandic, M. Golz, A. Kuh, D. Obradovic, T. Tanaka, Signal Processing Techniques for Knowledge Extraction and Information Fusion, Springer, 2008.

[4] J.W. Tukey, Exploratory Data Analysis, Addison-Wesley, 1977.

[5] N.E. Huang, Z. Shen, S. Long, M.C. Wu, H. Shih, Q. Zheng, N. Yen, C. Tung, H.H. Liu, The empirical mode decomposition and the Hilbert spectrum for nonlinear and non-stationary time series analysis, Proceedings of the Royal Society A 454 (1998) 903–995.

[6] R. Narayanan, Through wall radar imaging using UWB noise waveforms, in: IEEE International Conference on Acoustics, Speech and Signal Processing (ICASSP'08), 2008, pp. 5185–5188.

[7] C.M. Sweeney-Reed, S.J. Nasuto, A novel approach to the detection of synchronisation in EEG based on empirical mode decomposition, Journal of Computational Neuroscience 23 (1) (2007) 79–111.

[8] D. Looney, L. Li, T.M. Rutkowski, D.P. Mandic, A. Cichocki, Ocular artifacts removal from EEG using EMD, in: First International Conference on Cognitive Neurodynamics, 2007, pp. 831–835.

[9] T.M. Rutkowski, A.C. Francois Vialatte, D.P. Mandic, A.K. Barros, Auditory Feedback for Brain Computer Interface Management—An EEG Data Sonification Approach, Springer, Berlin, 2006.

[10] J.S. Smith, The local mean decomposition and its application to EEG perception data, Journal of The Royal Society Interface (2005) 443–454.

[11] Y. Wang, Z. He, Y. Zi, A demodulation method based on improved local mean decomposition and its application in rub-impact fault diagnosis, Measurement Science and Technology 20 (2009) 1–10.

[12] Y. Wang, Z. He, Y. Zi, A comparative study on the local mean decomposition and empirical mode decomposition and their applications to rotating

machinery health diagnosis, Journal of Vibration and Acoustics 132 (2) (2010) 1–10.

[13] D. Looney, D.P. Mandic, Multi-scale image fusion using complex extensions of EMD, IEEE Transactions on Signal Processing 57 (4) (2009) 1626–1630.

[14] S. Leslieand, M. Nhamoinesu, A tool for synthesizing spike trains with realistic interference, Journal of Neuroscience Methods 159 (1) (2006) 170–180.

[15] M.U.B. Altaf, T. Gautama, T. Tanaka, D.P. Mandic, Rotation invariant complex empirical mode decomposition, in: Proceedings of the IEEE International Conference on Acoustics, Speech, and Signal Processing (ICASSP'07), 2007, pp. 1009–1012.

[16] T. Tanaka, D.P. Mandic, Complex empirical mode decomposition, IEEE Signal Processing Letters 14 (2) (2007) 101–104.

[17] G. Rilling, P. Flandrin, P. Gongalves, J.M. Lilly, Bivariate empirical mode decomposition, IEEE Signal Processing Letters 12 (2007) 1–4.

[18] N. Rehman, D.P. Mandic, Multivariate empirical mode decomposition, Proceedings of the Royal Society A 466 (2117) (2010) 1291–1302.

[19] N. Rehman, D.P. Mandic, Empirical mode decomposition for trivariate signals, IEEE Transactions on Signal Processing 58 (3) (2010) 1059–1068.

Cheolsoo Park received the B.Eng. degree with Cum Laude honor in Electrical Engineering from Sogang University, Seoul, South Korea, in 2004, and the M.Sc. degree in Biomedical Department from Seoul National University, Seoul, South Korea, in 2006.

Currently, he is pursuing the Ph.D. degree in adaptive nonlinear signal processing at Imperial College London, London, UK. His research interests are mainly in the area of biomedical signal processing, brain computer interface (BCI) and time–frequency analysis.

David Looney received the B.Eng. degree in Electronic Engineering from University College Dublin, Ireland, in 2005. Currently, he is pursuing the Ph.D. degree in adaptive signal processing at Imperial College London, London, UK.

His research interests are mainly in the areas of data fusion and time–frequency analysis.

Marc Van Hulle is a Full Professor at the K.U.Leuven, Medical School, where he heads the Computational Neuroscience group of the Laboratorium voor Neuro- en Psychofysiologie. Marc Van Hulle received an M.Sc. degree in Electrotechnical Engineering (Electronics) and a Ph.D. in Applied Sciences from the K.U.Leuven, Leuven (Belgium). He also holds B.Sc.Econ. and MBA degrees. In 1992, he has been with the Brain and Cognitive Sciences Department of the Massachusetts Institute of Technology (MIT), Boston (USA), as a postdoctoral scientist. He has authored the monograph Faithful representations and topographic maps: from distortion- to information-based self-organization (John Wiley, 2000; also translated in Japanese), and 200 technical publications.

Dr. Van Hulle is an Executive Member of the IEEE Signal Processing Society, associate editor of IEEE Transactions on Neural Networks, Computational Intelligence and Neuroscience, and International Journal of Neural Systems. He is also member of the Program Committees of the Machine Learning in Signal Processing (MLSP) workshops, the International Conference on Intelligent Data Engineering and Automated Learning (IDEAL), International Conference on Informatics in Control (ICINCO), International Conference on Artificial Neural Networks (ICANN), International Conference on Computational Intelligence and Security (CIS), Workshop on Cognitive Information Processing (CIP), and the Workshop on Self-Organizing Maps (WSOM). His research interests include computational neuroscience, neural networks, computer vision, data mining and signal processing. In 2003, he received from Queen Margrethe II of Denmark the Doctor Technices degree, and in 2009 a Honory Doctoral degree from the Brest State University.

Danilo P. Mandic is a Reader in Signal Processing at Imperial College London. He has been working in the area of nonlinear adaptive signal processing and nonlinear dynamics. His publication record includes two research monographs titled Recurrent Neural Networks for Prediction (1st ed., Aug. 2001) and Complex-Valued Nonlinear Adaptive Filters: Noncircularity, Widely Linear and Neural Models (1st ed., Wiley, Apr. 2009), an edited book titled Signal Processing for Information Fusion (Springer, 2008) and more than 200 publications on signal and image processing. He has been a Guest Professor at K.U. Leuven Belgium, TUAT Tokyo, Japan, and Westminster University, UK, and a Frontier Researcher in RIKEN Japan.

Dr. Mandic has been a Member of the IEEE Technical Committee on Machine Learning for Signal Processing, Associate Editor for the IEEE Transactions on Circuits and Systems II, IEEE Transactions on Signal Processing, IEEE Transactions on Neural Networks, and the International Journal of Mathematical Modelling and Algorithms. He has produced award winning papers and products resulting from his collaboration with Industry. He is a Member of the London Mathematical Society.